Evaluation of Locomotion Performances for a Mecanum-wheeled Hybrid Hexapod Robot

E. C. Orozco-Magdaleno, F. Gómez-Bravo, E. Castillo-Castañeda, and G. Carbone

***Abstract*— Recently, research on hybrid mobile robots is attracting considerable interest due to the ability of these systems to perform service tasks in heterogeneous scenarios and irregular terrains. This paper proposes a specific hybrid locomotion configuration, which combines legs and Mecanum-omniwheels into a six-legged hexapod robot. Theoretical backgrounds and open issues are addressed by considering some challenging problems such as: gait planning, modeling omnidirectional motion and designing a control architecture for combining locomotion modes. The paper demonstrates suitability, feasibility and successful performance of the proposed locomotion strategies and presents experimental results and novel scientific contributions regarding the motion of hybrid mobile robots.**

***Index Terms*— Robots, Mobile robots, Mobile robot kinematics, Mobility & locomotion.**

I. Introduction

MOBILE robots are devices with self-locomotion capability that allow autonomous motion in structured and unstructured environments [1]. This type of devices usually extends the range of robots' action, initially limited by a mechanical structure anchored at one of its extremities, [2]. Mobile robots are mainly designed to carry out different tasks for human being, which are difficult to perform in heterogeneous environments, with obstacles and uneven terrains [3], [4]. Walking robots (WR) have been designed to solve the problem of displacement over irregular terrains that can be challenging for conventional wheeled vehicles. Particular cases of WR are hexapod robots [5], [6], [7]. This kind of robots can easily adapt its locomotion mechanism to the terrain features by adjusting the gait patterns, footfall path or footholds [8], [9]. However, wheeled robots can have a better performance especially in terms of speed and energy efficiency on flat surfaces. Accordingly, a hybrid locomotion configuration can combine two or more different kinds of locomotion, to benefit of their combined advantages in heterogeneous scenarios. Hybrid hexapod robots are wheeled-legged robots that move by walking on legs and/or also by rolling on wheels [10, 11]. Thus, each hybrid leg consists of a leg with a wheel attached at its extremity. There are several advantages of six wheeled-legged robot in comparison with traditional 4-wheeled or 6-legged mobile platforms. On one hand, 6-wheeled vehicles provide more robust driving than 4-wheeled vehicles; on the other hand, robots with legs and wheels can move faster and more efficiently on smooth surfaces in comparison with robots moving only on legs. Moreover, this solution offers the advantage of having a redundant 6-wheel system, which allows moving even if one or two wheels fail.

Cassino Hexapod III is the most recent version of the Cassino Hybrid Hexapod Robot series [2, 12, 13]. This current version of the hexapod has been carefully re-designed and re-engineered as compared with the previous ones. Among other new features, its leg extremities have been designed with a customized solution that is based on the Mecanum-wheel concept. The addition of this type of wheels allows new omni-directional locomotion strategies, which were not feasible with other hybrid hexapods [10, 11, 12]. The vehicle can move in any direction without changing robot or wheels orientations (as is the case of robot with steerable wheels).

Regarding Cassino Hexapod III, this paper addresses some challenging problems, not approached until now, in terms of motion requirement, modeling complexity and degrees of freedom. The main and innovative contributions of this work lie in modeling the locomotion capabilities of the robot and implementing various modes of operation. Moreover, gait planning, and obstacle overcoming cases are also analyzed. The article discusses navigation issues by implementing different strategies of motions for legged-, wheeled-, omni-wheeled-, and combined wheeled-legged-locomotion modes. It also illustrates a new control architecture, developed so that remote access, and the addressed motion strategies can be implemented. The paper evaluates the robot performance through several laboratory tests. A specific experimental set up is proposed to obtain the robot´s performance in terms of feasibility, speed, and energy efficiency.

II. Navigation of a Hybrid Hexapod

The navigation of a hybrid hexapod involves the solution of different problems including trajectory planning, collision avoidance and locomotion control.

E. C. Orozco-Magdaleno is with CICATA (Research Center on Applied Science and Advanced Technology), Queretaro Unit, of the IPN (National Polytechnic Institute), Queretaro, Mexico. (e-mail: eorozcom1600@alumno.ipn.mx)

F. Gómez-Bravo is with the Electronic Systems and Mechatronics research group of the University of Huelva, Huelva, Spain. (e-email: fernando.gomez@diesia.uhu.es).

E. Castillo-Castañeda is with CICATA (Research Center on Applied Science and Advanced Technology), Queretaro Unit, of the IPN (National Polytechnic Institute), Queretaro, Mexico. (e-mail: ecastilloca@ipn.mx)

G. Carbone is with the Dept. of Mechanical, Energy and Management Engineering, DIMEG, of the University of Calabria, Rende, Italy. (e-mail: giuseppe.carbone@unical.it) and with TU Cluj-Napoca, Romania.

This article has been accepted for publication in a future issue of this journal, but has not been fully edited. Content may change prior to final publication. Citation information: DOI 10.1109/TMECH.2020.3027259, IEEE/ASME Transactions on Mechatronics

Usually, trajectory planning and collision avoidance strategies are regarded in a first phase by generating a collision-free navigation path. In a second phase, a suitable locomotion strategy makes the robot follow the planned path.

Trajectory planning algorithms generate a path from an initial to a final target point, passing through predefined via-points, as reported in [14]. Collision avoidance strategies generally consider proximity sensor data to modify the original trajectory in order to avoid collisions with non-modeled obstacles, such as addressed in [1]. A general approach for hybrid hexapod robot's navigation is based on the definition of the precision points and via-points by referring to the robot´s Centre of Mass (CoM), [15], as it is shown in the scheme of Fig. 1. The trajectory between via-points in Cartesian space can be further decomposed by using splines and knots, such is reported in [14]. Thus, navigating from A to B, Fig. 1, implies moving the robot's CoM through the via points and the knots. This motion can be implemented by using wheeled, legged, or wheeled-legged combined locomotion, depending on the kind of surface and the obstacles that are detected in the nearby environment.

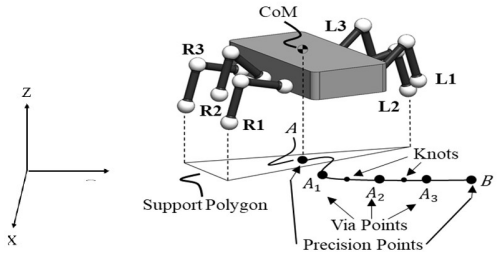

Fig. 1. A scheme with main navigation parameters for a hexapod robot.

III. Locomotion Issues

The locomotion of a hybrid hexapod robot involves a complex combination and coordination of wheel motions and gait executions. Accordingly, in the following we address the main peculiarities of the gait planning, the Mecanum-wheel locomotion and the hybrid locomotion.

A. Gait Planning

One of the most significant problems for legged locomotion is stability. This issue can be categorized into two kinds: dynamic (like running and hopping) and static (like walking). In static stability, the vertical projection of the CoM of the robot must always be within the support polygon of the legs which have ground contact, Fig. 1. Dynamic stability is needed when CoM is outside or on the border of the support polygon. In that situation, the robot will fall over when no additional forces and movement are made by the legs, [16], [17]. Walking pattern selection depends on several factors such as robot body shape, terrain type; and performance requirements like stability, speed, mobility and power consumption, [17]. In [16] a gait classification is reported. It proposes a classification with two main modes: periodic and non-periodic gaits. A periodic gait is when the legs always have the same mode points (number of points that one leg needs to follow during a locomotion cycle), and all the leg cycles have the same duration. Periodic gaits repeat the same sequence of steps every cycle [12]. In regular gaits, all the legs have the same duty cycle β (time duration of movement of one leg during the locomotion cycle [12]). A gait is defined as symmetric when the motion of the legs of any right-left pair is exactly half a cycle out of phase. Thus, a wave of protractions runs from posterior to anterior; contralateral legs of the same segment alternate in phase; protraction time is constant; retraction time decreases as walking frequency increases; the intervals between steps of ipsilateral adjacent legs are constant, while the interval between the foreleg and hind leg steps varies inversely with frequency. The most prevalent and used wave gaits in hexapod walking robots are metachronal, ripple and tripod gaits. These gaits are shown in Fig. 2, Fig. 3 and Fig. 4, respectively, [12]. In the reported schemes, beneath each leg, the gray color and the tiny circle indicate the leg in swing phase (not touching the ground).

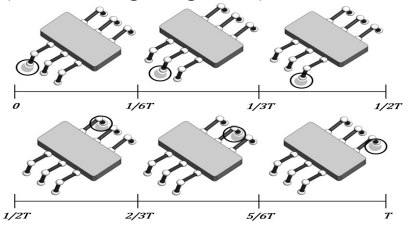

Fig. 2. A scheme of metachronal gait.

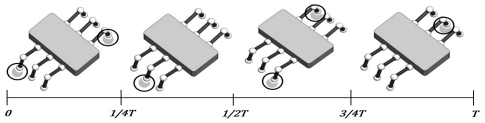

Fig. 3. A scheme of ripple gait.

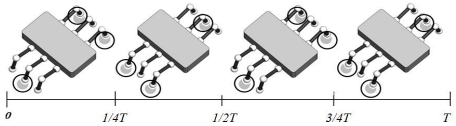

Fig. 4. A scheme of tripod gait.

Metachronal gait, Fig. 2, is adopted by a hexapod robot when it moves slowly. This kind of gait can be described as a back to front propagating wave. It means that first the limbs move on the right side and then on the left side. In the metachronal gait, all legs on one side are moved forward in succession, starting with the rear-most leg. Then, this is repeated on the other side. Since only one leg of the robot is ever lifted at a time, with the other five legs being down, the robot is always in a highly stable posture. This wave gait is considered the most stable gait. Ripple gait, Fig. 3, is used by hexapod robots to move with a medium speed where each foot is on the ground during a fraction of the cycle time. During the ripple gait, L1 and R3 legs (see Fig. 1) start to move together, then, after one quarter of period moves R2 leg, more a quarter of a cycle, R1 and L3 legs begin to move, and finally, after more a quarter of the cycle, L2 leg moves. This wave gait is the next most stable, since only two legs are ever off the ground at the same time. Tripod gait, Fig. 4, is the best-known walking gait for hexapod robots [12]. It consists of the front-back legs on one side and the middle leg on the opposite side. For each tripod, the legs are lifted, lowered, and moved forwards and backwards synchronously [12]. During the

This article has been accepted for publication in a future issue of this journal, but has not been fully edited. Content may change prior to final publication. Citation information: DOI 10.1109/TMECH.2020.3027259, IEEE/ASME Transactions on Mechatronics

walking locomotion, the hexapod robot uses two tripods like a biped stepping from one foot to the other: the weight is simply shifted alternately from one tripod to the other. Three legs are always on the ground, so it is statically and dynamically stable, and suitable for high speed walking over flat surfaces.

B. *Mecanum-wheels Locomotion*

Omni-directional wheeled robots have been traditionally designed with four omni-wheels, [18]. An omni-wheel is a wheel with rollers attached to its circumference. Each roller rotates about an axis that forms an angle α with the plane of the disk. This allows them to be driven with full rotations, but also to slide laterally. A Mecanum-wheel is an omni-wheel where the angle α is defined at 45°, Fig. 5a), [19]. These wheels have additional kinematical possibilities in comparison with conventional wheels. By varying the speed and the direction of rotation of each wheel, a robot can have a translational displacement in any direction, as well as arbitrary turns and rotations on the spot. The Mecanum-wheeled robots can be modelled by considering non-holonomic constraints [20]. A general solution approach, must consider a general kinematical scheme such as proposed in Fig. 5b) and c), [18].

This scheme represents the motion of a Mecanum-wheel that moves in the x-y plane. Fig. 5b) illustrates the wheel and a roller that touches that plane at a point G. This point is always under the main wheel axis s1. Thus, motion is generated by two rotational movements around axes s1 and s2, Fig. 5c). The first one, s1, goes through the point C, Fig. 5b), being orthogonal to the vertical plane of the wheel. Around this axis a rotation with velocity $\vec{\omega}_w$, is generated by a motor. The roller passively spins around s2, with velocity $\vec{\omega}_r$, due to the wheel movement. According to [18], and considering the roller's dimension, the velocity of G can be calculated as:

$$\vec{V}_G = \vec{V}_C + \overrightarrow{\omega_w} \times (\vec{r} + \vec{l}) + \overrightarrow{\omega_r} \times \vec{l} \qquad (0)$$

where $\vec{l}$ and $\vec{r}$ are defined in Fig. 5b). By assuming ideal non-slipping conditions, $\vec{V}_G$=0, [18], (0) will determine $\vec{\omega}_w$ and $\vec{\omega}_r$ for achieving a desired, $\vec{V}_c$, the velocity of point C. The robot has been designed to roll mostly on flat surfaces, so, apart from the non-slipping conditions, others wheel-terrain interactions are considered negligible.

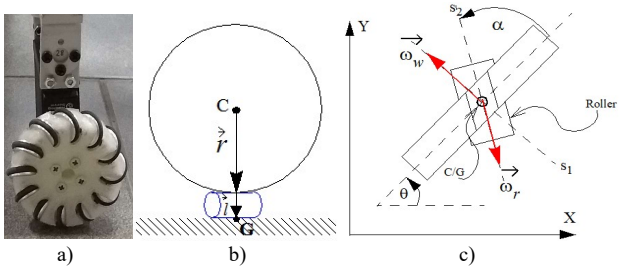

Fig. 5. Mecanum-wheel: a) detail of a Mecanum-wheel from Cassino Hexapod III; b) vertical representation; c) horizontal representation.

C. *Hybrid Locomotion*

Wheeled-legged hexapod robots are intended to move in a variety of situations. One example of a challenging scenario can happen when the robot is rolling over a flat surface, a small obstacle appears in front of robot, and the robot needs to overcome the object by just lifting one, two or more legs. To execute this maneuver, the robot has to identify when it is convenient to start the legged locomotion, what legs need to be operated and what leg motion pattern needs to be performed. Particularly, for this scenario this paper implements a bio-inspired locomotion, generated by means of a genetics approach as is presented in [21].

IV. CASSINO HEXAPOD III CASE STUDY

Cassino Hexapod Robot III, Fig.6a), is the latest version of Cassino Hexapod family [13], a series of hybrid wheeled-legged mobile robots that has been conceived and built at LARM laboratory [2, 12]. It has a body shape that can fit into a box of 375 x 230 x 200 mm, Fig.6a) and b), that allows to have two frontal legs, two lateral legs (one on each side), and two rear legs; all of them in frontal orientation. Each hybrid leg has: a Mecanum-wheel as End-Effector (EE) Fig. 5a), and Fig.6c); two servomotors to move and orientate the leg; and one continuous rotation servomotor for actuating the Mecanum-wheel, Fig.6a). The arrangement of legs has been chosen to mimic mammals in terms of motion and obstacle avoidance strategies. The wheels have been specifically designed to allow a proper integration with the leg body, a reduced footprint, and a minimum actuator size. Besides wheels, Cassino Hexapod III was redesigned for increasing autonomy and size of negotiable obstacles by about 30%.

The control architecture, Fig.6d), is mounted inside the robot's body, consisting of an Arduino MEGA ADK as the main controller, and a Mega Servo Shield for connecting the servomotors. The robot uses twelve metal gear servomotors (RDS3115) and six continuous rotation servomotors (AS3103) as actuators. Data acquisition has been obtained with a dedicated LabView virtual instrument and a data acquisition board National Instrument NI-DAQ 6009. The experimental set up includes an ultrasonic sensor, HC-SR04, for measuring linear displacement and velocity; a current sensor, ACS712, is

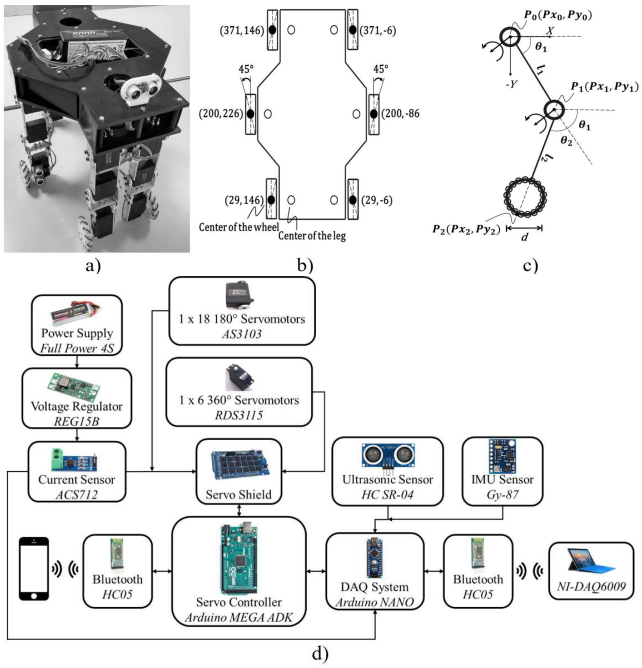

Fig. 6. Cassino Hexapod III: a) prototype; b) main robot´s dimensions; c) kinematic diagram of one leg, d) control architecture.

This article has been accepted for publication in a future issue of this journal, but has not been fully edited. Content may change prior to final publication. Citation information: DOI 10.1109/TMECH.2020.3027259, IEEE/ASME Transactions on Mechatronics

used to obtain the power consumption; a IMU sensor, GY-87, is used to calculate angular displacements (Roll, Pitch and Yaw), and the linear accelerations in the local reference frame. The ultrasonic sensor, HCSR04, has an operation range from 2 mm to 4 m with a measuring angle of 15° and a declared accuracy of 0.1% full scale (F.S.) and a minimum resolution of 0.35 mm. The IMU GY-87 board has a MPU6050 chip which includes a 3-axis gyroscope and a 3-axis. The accuracy of the gyroscope is about 0.1 % F.S. and the accuracy of the accelerometer is about 3% F.S. with the full scales set at ± 250°/s and ± 2 g, respectively. The current sensor ACS712 can measure AC/DC currents up to 20 A with an accuracy of 1.5%. F.S. and a resolution of 66 mV/A. A customized board has been designed and built to integrate Arduino boards, servomotors, and all the onboard sensors. It includes a Bluetooth connection that allows complete remote interaction with the robot for both data analysis on a remote device (through an Arduino NANO acquisition system and a PC acquisition board), and for the use of a specifically designed Java user interface that runs on any Android smartphone.

A. Leg's Inverse Kinematics

Inverse kinematic model of one leg is solved to calculate a proper path of the robot during a walking mode. Thus, inverse kinematics allows to know the angular position of each joint to follow the desired path by using the Cartesian coordinate of EE. This is solved by applying a geometric method for an elbow up solution, as described in [12], by means of the following equations, Fig. 6c):

$$Q = \frac{{Px_2}^2+{Py_2}^2-{l_1}^2-\left(l_2+\frac{d}{2}\right)^2}{2l_1l_2} \quad (0)$$

$$\theta_2 = -arctan\left(\frac{\sqrt{1-C^2}}{Q}\right) \quad (0)$$

$$\theta_1 = arctan\left(\frac{Px_2}{-Py_2}\right) - arctan\left(\frac{l_2\,sin\,\theta_2}{l_1+l_2\,cos\,\theta_2}\right) \quad (0)$$

where l_1 and l_2 are the lengths of the links of a leg, Px_2 and Py_2 are the x and y coordinates of the leg endpoint P_2, d is the diameter of wheel, and θ_1 and θ_2 the angles of the leg´s joints.

B. Wheels kinematics

One of the most relevant characteristics of Mecanum-wheels is their capacity of moving without constraining the motion direction. For example, the robot can slide to the right or to the left without changing orientation. However, Mecanum-wheels can still perform locomotion strategies like a conventional nonholonomic robot. Thus, it is necessary to analyze and model both omnidirectional and nonholonomic locomotion.

1) Omnidirectional locomotion model

The motion of the robot is characterized by the velocity ($\vec{V}_0$) of the origin of the local reference frame Σ_L and the angular velocity $\vec{\Omega}$ of the robot body. If one considers a planar motion, $\vec{\Omega}$ has only a z component and V_0 has only x and y components, Fig. 7a). Thus, when the robot moves with a planar omni-directional motion, given any value of Ω_z, the linear velocity can have any arbitrary module $|V_0|$ and any arbitrary orientation (γ) in Σ_L, Fig. 7a). Let be Ci the central point of the wheel i, defined was shown in Fig. 5b).

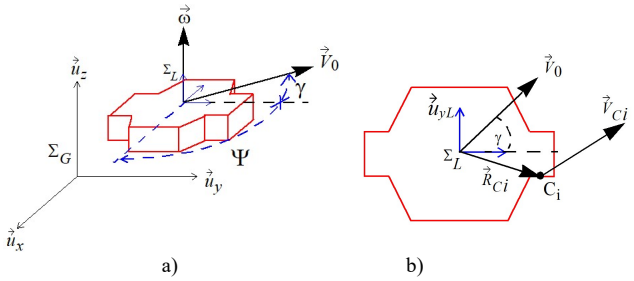

a) b)

Fig. 7. Kinematic diagram of the omnidirectional hexapod: a) planar motion of the robot's body; b) velocity of point Ci (point C of wheel *i*, see also Fig 5).

According to Fig. 7a) and b), the velocity of point Ci ($\vec{V}_{Ci}$) is:

$$\vec{V}_{Ci} = \vec{V}_0 + \vec{\Omega} \times \vec{R}_{Ci} \quad (0)$$

Moreover, from (0), and assuming non-slipping conditions, the following expression can be obtained:

$$\vec{V}_{Ci} = -\overrightarrow{\omega_{wi}} \times \left(\vec{r} + \vec{l}\right) - \overrightarrow{\omega_{ri}} \times \vec{l} \quad (0)$$

where the subscript *i* indicates that the magnitudes refer to the wheel *i*. When all vectors are expressed in Σ_L, one can define:

$$\vec{V}_0\big|_L = [|V_0| \cdot cos(\gamma) \quad |V_0| \cdot sin(\gamma) \quad 0]^T \quad (0)$$

$$\vec{\Omega}\big|_L = [0 \quad 0 \quad \Omega_z]^T \quad (0)$$

$$\vec{R}_{Ci}\big|_L = [R_{Cix} \quad R_{Ciy} \quad 0]^T \quad (0)$$

$$\vec{r}|_L = [0 \quad 0 \quad -r]^T, \vec{l}\big|_L = [0 \quad 0 \quad -l]^T \quad (0)$$

$$\overrightarrow{\omega_{wi}}|_L = [0 \quad \omega_{wi} \quad 0]^T \quad (0)$$

$$\overrightarrow{\omega_{ri}}|_L = [\omega_{ri} \cdot \cos(\alpha_i) \quad \omega_{ri} \cdot \sin(\alpha_i) \quad 0]^T \quad (0)$$

where R_{Cix} and R_{Ciy} are the coordinates *x* and *y* of the center of the wheel *i* in Σ_L and α_i represent the wheel's rollers orientation. Then, by equating the right side terms of (0) and (6), and using expressions (0) to (12) ω_{wi}, can be expressed:

$$\omega_{wi} = \frac{1}{(r+l)} \cdot \left[1 \;\; tan(\alpha_i) \;\; tan(\alpha_i) \cdot R_{Cix} + R_{Ciy}\right] \cdot [A] \quad (0)$$

$$A = [|V_0| \cdot cos(\gamma) \quad |V_0| \cdot sin(\gamma) \quad \Omega_z]^T \quad (0)$$

Considering that the robot has six wheels, a general expression can be found for defining $[\omega_{wi}]$ as:

$$[\omega_{wi}] = [J_{om}] \cdot [A] \quad (0)$$

where *i= 1...6,* is the number of the wheels, see Fig. 9, and $[J_{om}]$ is a 6x3 matrix built by stacking the six equations for ω_{wi} obtained from (13). For Cassino Hexapod III, the values that define each row of $[J_{om}]$ are presented in Table I. By means of equation (0) the values of the rolling velocities of the six Mecanum-wheels are determined so that the robot moves following any direction γ (in the local reference frame) with an arbitrary angular velocity Ω_z, and speed $|V_0|$.

TABLE I
PARAMETERS OF CASSINO HEXAPOD III

i	1	2	3	4	5	6
α_i (rad)	$-\frac{\pi}{4}$	$\frac{\pi}{4}$	$-\frac{\pi}{4}$	$\frac{\pi}{4}$	$-\frac{\pi}{4}$	$\frac{\pi}{4}$
R_{Cix} (cm)	17.1	0	−17.1	17.1	0	−17.1
R_{Ciy} (cm)	7.6	15.6	7.6	−7.6	−15.6	−7.6

This article has been accepted for publication in a future issue of this journal, but has not been fully edited. Content may change prior to final publication. Citation information: DOI 10.1109/TMECH.2020.3027259, IEEE/ASME Transactions on Mechatronics

2) Nonholonomic locomotion model

Robots on Mecanum-wheels can also be operated as a classical differential-drive platform. In this case, robot's kinematics must accomplish the traditional nonholonomic constraint [1]:

$$V_{0x} \cdot sin\,\Psi - V_{0y} \cdot cos\,\Psi = 0 \quad (0)$$

$$\vec{V}_0 \cdot \vec{u}_{yL} = 0 \quad (0)$$

where V_{ox} and V_{oy} are the components of $\vec{V}_0$ in the global reference frame, and Ψ is the robot's heading, see Fig. 7a). Note that (0) and (0) represents the same nonholonomic condition, but particularly (0) is written in the robot's local frame, where $\vec{u}_{yL}$ is the unitary vector, of the Y axis, in Σ_L, see Fig. 7b). Then, (0) is accomplished if γ satisfies (0):

$$\gamma = k \cdot \pi, k = 0,1,2 \ldots \quad (0)$$

Thus, by substituting (0) in (0) the robot kinematics can be reformulated similar to a classical differential-drive model:

$$[\omega_{wi}] = [J_{non}] \cdot \begin{bmatrix} V_0 \\ \Omega_z \end{bmatrix} \quad (0)$$

where V_0 is the projection of $\vec{V}_0$ on the X axis of Σ_L and $[J_{non}]$ is a 6x2 matrix built from the values of α_i, R_{Cix} and R_{Ciy}. By applying (0), the rolling velocities of the six Mecanum-wheels are determined so that the robot motion accomplishes the nonholonomic constraint expressed in (0) and (0).

V. Locomotion Strategies with Cassino Hexapod III

This section outlines the most significant locomotion strategies for Cassino Hexapod III including legged locomotion with tripod gait, wheeled/omniwheeled locomotion and combination of wheels and legs.

A. Legged Locomotion

Legged locomotion planning starts by computing the desired locomotion path for one leg by using the inverse kinematics equations (0), (0) and (0). As a result, for example, a pentagonal path is shown in Fig. 8, enabling a step with length equal to 80 mm and height equal to 40 mm that can be suitable for overcoming small obstacles. A tripod gait strategy can be implemented for properly displacing the robot. For this gait is necessary to synchronize the support polygon or support triangle with the motion of the pentagonal path by considering the accessible distance to move each leg, which will change at each leg movement. Moreover, in the tripod gait three legs define the support triangle as they are in contact with the ground simultaneously. Special attention must be given to synchronizing the robot motion, because while the robot's support triangle moves on a plane (support phase), the other tripod sequence moves on air (swing phase).

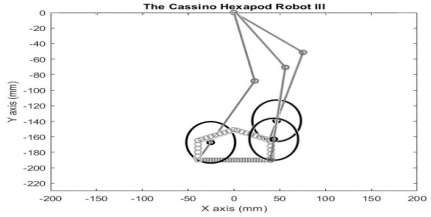

Fig. 8. Pentagonal path for one step with Cassino Hexapod III. (grey circles represent the positions during a full walking cycle of a point, which is tangent to the wheel and located along the prolongation of the last link of the leg).

This allows the robot to have turns or slips during a straight walk if these tripod sequences are not well synchronized. Hence, it is convenient considering different foot hold positions of each leg, so the triangle support displacement will be smooth, Fig. 9. One may notice that each leg's foot hold must move from positions 0 to 3, passing through positions 2 and 3, Fig. 9. Assuming to move along a flat surface, the wheel-terrain interaction is here considered on basis of a purely kinematic model.

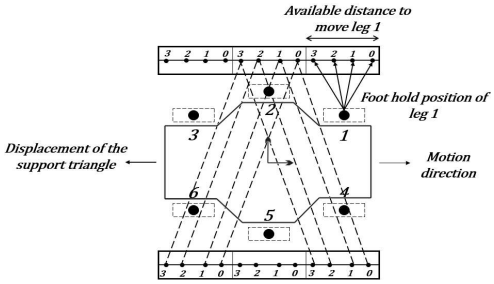

Fig. 9. The foothold position of legs with triangular support pattern showing the tripod gait having a stability margin.

B. Wheeled Locomotion

A characteristic of Cassino Hexapod III is the capability to move either following an omnidirectional or a nonholonomic constrained motion. Accordingly, Fig. 10 shows two examples of collision avoidance maneuvers using different rolling modes. Fig. 10a) displays a traditional differential movement; the robot's linear velocity is always perpendicular to the wheels' axes. Instead, in Fig. 10b) the robot's linear velocity is always parallel to the wheels' axes. This can only be achieved with omnidirectional movements. Usually Mecanum-wheels are implemented in four wheels set ups, this simplifies the control and maneuverability. However, since Cassino Hexapod III has a rectangular body shape, this type of movements can be configured in four and six Mecanum-wheel operating modes. The advantage of rolling with six instead of four wheels will be shown in the experimental section where two legs are lifted to obtain four wheels set up.

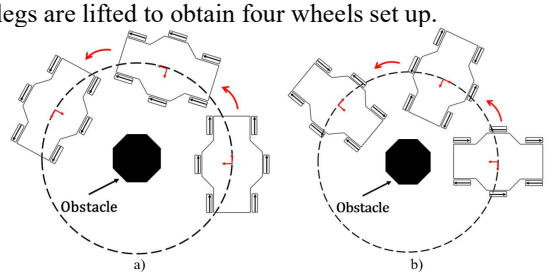

Fig. 10. Obstacle avoidance by wheeled locomotion: (a) nonholonomic motion; (b) omnidirectional motion.

C. Wheeled-legged Locomotion

The wheeled-legged hybrid configuration of Cassino Hexapod III allows to combine legs and wheels motions. It implies that during a displacement with wheels, the robot can also move one or more legs for achieving the overcoming of small obstacles. Proper synchronization of the movements will allow to achieve complex motions, including bio-inspired obstacle overcoming with a horse-like step, Fig. 11a); a human-like backward step, Fig. 11b); a human-like forward step; Fig. 11c), or a bird-like step, Fig. 11d), [21].

This article has been accepted for publication in a future issue of this journal, but has not been fully edited. Content may change prior to final publication. Citation information: DOI 10.1109/TMECH.2020.3027259, IEEE/ASME Transactions on Mechatronics

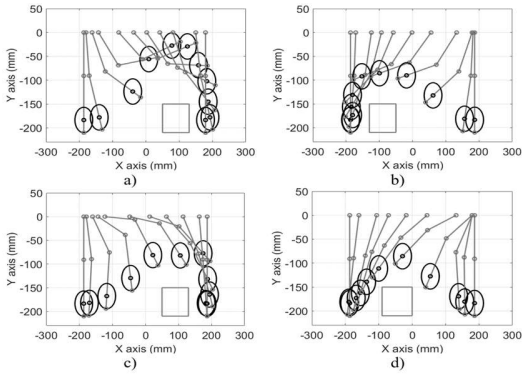

Fig. 11. Gaits to overpass obstacles with Cassino Hexapod III, in a wheeled-legged motion: (a) Horse-like; (b) human-like backward; (c) human-like forward; (d) bird-like step.

VI. Experimental Setup and Test Modes

Several operation modes have been implemented with Cassino Hexapod III as based on the concepts presented in the previous sections. A detailed list of all the test modes has been reported in Table II, which also indicates the input and output parameters. For example, the input parameters for the rolling mode with four wheels are the angular speeds of each wheel ω_{1-4}, while the corresponding output parameters are the evolution of the Euler's angles Θ, Φ, Ψ, see Fig. 12a), the acceleration's components a_X, a_Y, a_Z, as well as the average of the robot's power consumption P_w and linear speed V_0.

These variables were chosen to evaluate and create a performance profile of the robot. Thus, the power consumption allows to evaluate the autonomy and energy performance of the robot. The linear displacement and velocity allow to obtain the main parameters of the wheeled, legged and hybrid locomotion. The angular displacements allow to obtain the real track of the center of mass. Also, from these values the vibrations of the robot can be obtained to improve the mechanical construction or the velocity profiles.

TABLE II
Tested Operation Modes with Cassino Hexapod III

Type of locomotion	Test	Motion type	Input	Output
Rolling in straight displacement	Rolling with four wheels	Forward Backward	ω_{1-4}	Θ, Ψ, Φ a_X, a_Y, a_Z P_w V_0
	Rolling with six wheels		ω_{1-6}	
Legged locomotion	Walking with six legs	Forward Backward	P_x, P_y	
Rolling in curved displacement	Rolling with six wheels	Nonholonomic motion Omnidirectional motion	ω_{1-6}	Θ, Ψ, Φ a_X, a_Y, a_Z P_w
Wheeled-legged locomotion	Overcoming obstacles	Horse-like gait Human-like forward gait Human-like backward gait Bird-like gait	ω_{1-6} P_x, P_y	
	Walking and Rolling	Walking forward, turning by Rolling, and walking, bacward	ω_{1-6} P_x, P_y	

An amount of approximately 100 tests have been carried out. Experimental tests have been all arranged with the following procedure: 1) start of the electronics and sensor data collection; 2) wait 1 second to stabilize sensor measurements in robot stand still conditions; 3) perform test; 4) wait some time to stabilize sensor measure in robot stand still conditions. A customized low-pass filter has been implemented to remove high frequency noise. The statistical analysis of the results comprises the mean and the standard deviation (σ) of the measured values for each of the considered variables. The aim of the test is to outline all the feasible locomotion possibilities of the proposed design. Further, automatic, selection of the locomotion strategies can be achieved by using the sensory feedback. For example, if the robot detects a small obstacle, it may change from wheeled to legged locomotion. For this purpose, multiple sensors can be used. So far, we have successfully tested ultrasonic sensors, and IMU sensors for accelerations and gyro feedback. Likewise, cameras, and LIDAR can be used for obstacle avoidance.

Table III provides a summary of the statistical values (average and σ) of the tests with Cassino Hexapod III in all different experiments. The robot is controlled via Bluetooth by using a developed Android interface, Fig. 12b). This interface has different buttons for controlling the robot. It has four checkboxes to select the operation mode of the robot: nonholonomic, walking, omnidirectional and hybrid. This last mode has one button to select four different overcoming paths.

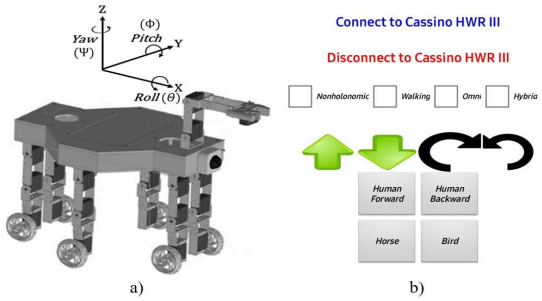

Fig. 12. Cassino Hexapod III a) local reference frame; b) android interface.

TABLE III
Summary of the Statistical Values of the Different Tests

Locomotion	V_0 [cm/s]	Max. Ψ [°]	Max. a_Z [m/s²]	P_w [W]
Straight displacements	14.16 σ=0.088	1.26 σ=0.099	7.01 σ=0.091	4.73 σ=0.093
Legged	2.22 σ=0.111	1.10 σ=0.107	0.89 σ=0.094	7.42 σ=0.096
Omni-directional	22.00 σ=0.104	324.1 σ=0.098	1.38 σ=0.092	12.82 σ=0.095
Wheeled-legged	14.55 σ=0.106	1.88 σ=0.092	4.09 σ=0.100	7.30 σ=0.105

A. Rolling in Straight Displacement

The first test compares rolling modes on four wheels (lifting the middle legs to correctly balance the weight distribution) and on six wheels. An example of a displacement on 4 wheels is shown in Fig. 13. Rolling velocities are determined from (0) . Nevertheless, due to wheels slippage, an offset in some wheels is needed. The average rolling velocity on four wheels is 2.95 rad/s, and on six wheels 3.07 rad/s.

This article has been accepted for publication in a future issue of this journal, but has not been fully edited. Content may change prior to final publication. Citation information: DOI 10.1109/TMECH.2020.3027259, IEEE/ASME Transactions on Mechatronics

a) b) c)

Fig. 13. Photo sequence of the tested rolling mode in forward direction with four wheels: a) t = 0 s; b) t = 7 s; c) t = 10 s.

Experimental results are presented in Fig. 14, for a four wheeled locomotion, and in Fig. 15, for a six wheeled locomotion. The measured average linear velocity of the robot in the four wheels mode is 13.66 cm/s and 14.67 cm/s on six wheels. The robot's angular change is represented by the evolution of Ψ, Fig. 14b), since it corresponds to the angular movement over the robot's Z axis. The final angular deviation is 1.93°. The other two angular variations in Roll and Pitch, correspond to small vibrations due to surfaces irregularities in the floor. These small vibrations can be observed in Fig. 14c). It may be noted that a_Z is about 10 m/s^2 since the sensor also senses the acceleration of gravity. Thus, the maximum linear acceleration over Z axis is 5.26 m/s2. This acceleration is also interpreted as a vibration during the test. The average power consumption in the four wheels mode is 4.11 W, with a consumption peak of 5.35 W.

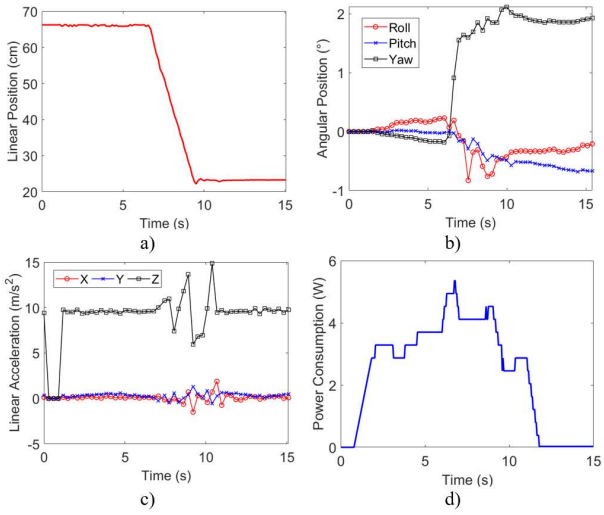

Fig. 14. Test results in four wheels rolling mode: a) Reached distance; b); Θ, Ψ, Φ ; c) a_X, a_Y, a_Z; d) power consumption.

Table IV compares the averaged measured values, and standard deviations (σ) of both rolling modes. It can be observed that the robot has a lower power consumption by using four wheels, 1.24 W less, and a small linear acceleration in the Z axis, 3.51 m/s^2 less, however it also has a larger final angular deviation in Yaw, 1.34 ° more, with a smaller linear velocity. These results show that during linear displacement the robot keeps orientation better with six than with four wheels. Therefore, the robot can have a better performance by using six wheels than with four wheels (higher linear velocity with minor angular deviation), this at cost of a small increase in power consumption and vibrations.

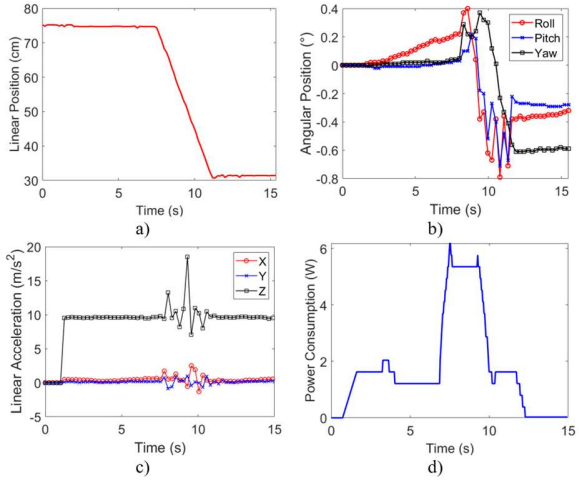

Fig. 15. Test results in six wheels rolling mode: a) Reached distance; b) Θ, Ψ, Φ ; c) a_X, a_Y, a_Z; d) power consumption.

TABLE IV
STATISTICAL RESULTS OF WHEELED LOCOMOTION TESTS.

Test mode	V_0 [cm/s]	Max. Ψ [°]	Max. a_Z [m/s^2]	P_w [W]
4 wheels	13.66 σ=0.088	1.93 σ=0.100	5.26 σ=0.097	4.11 σ=0.097
6 wheels	14.67 σ=0.112	-0.59 σ=0.102	8.77 σ=0.102	5.35 σ=0.112

B. *Legged Locomotion*

Legged locomotion has been implemented by using a tripod gait. For this purpose, the robot's controller has been programed so that the legs follow a pentagonal path for one forward step. Also, it also synchronizes the two tripod gaits, the one with the support triangle (in ground contact) and the one that is going forward (in the air), Fig. 16. Thus, the robot does not lose stability and equilibrium. For a better performance during the test, the wheels are blocked by their servomotors to avoid any slip derived from the external loads.

Experimental results are presented in Fig. 17, where the average linear velocity is 2.22 cm/s. As in the last section, the small angular variations on Pitch and Roll correspond to small lateral movement of the robot body during the walk. Table V summarizes the statistical results (averages and σ) of this test mode. The increasing power consumption, compared with the wheeled locomotion, is due to the continuous activation of all servomotors , and the high peaks happen when motion starts again after rest. One can also note that the wheeled locomotion has a better performance over flat surfaces, as expected.

TABLE V
STATISTICAL RESULT OF THE LEGGED LOCOMOTION TESTS.

V_0 [cm/s]	Max. Ψ [°]	Max. a_Z [m/s2]	Pw [W]
2.22 σ=0.092	1.10 σ=0.089	0.89 σ=0.103	7.42 σ=0.096

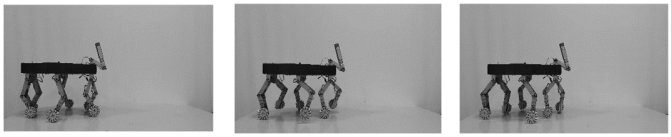

a) b) c)

Fig. 16. Sequence of the tested walking mode by giving one forward step: a) t = 0s; b) t = 4; c) t = 10s.

This article has been accepted for publication in a future issue of this journal, but has not been fully edited. Content may change prior to final publication. Citation information: DOI 10.1109/TMECH.2020.3027259, IEEE/ASME Transactions on Mechatronics

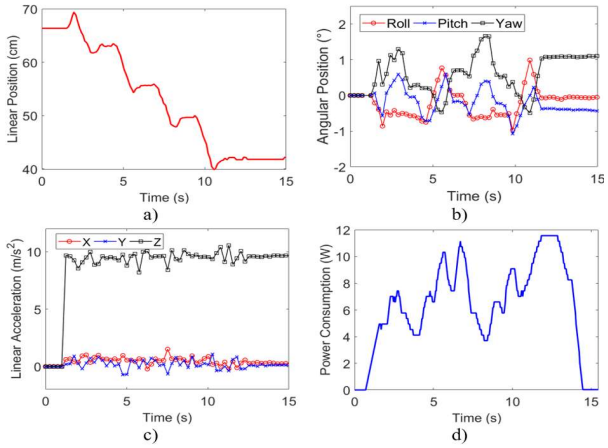

Fig. 17. Test results for the walking mode with tripod gait locomotion: a) Reached distance; b) Θ, Ψ, Φ ; c) a_X, a_Y, a_Z; d) power consumption

C. *Rolling in Curved Displacement*

These tests are aimed at showing the capability of the robot to reproduce curved trajectories, either following a classical nonholonomic motion, Fig. 18a), or an omnidirectional behavior by implementing a transverse motion, Fig. 18 b). For this purpose, equations (0), omnidirectional, and (0), nonholonomic, have been applied to calculate the rolling speed of each Mecanum-wheel. In both cases the robot follows a circular trajectory, whose radius is 30 cm, with a reference linear velocity, V_0, of 30 cm/s for nonholonomic motion and 22 cm/s for omnidirectional behavior. The wheels' angular speeds are reported in Table VI. Experimental results for nonholonomic and omnidirectional motions are reported in Fig. 19 and, Fig. 20 respectively. Linear accelerations for both tests are shown in Fig. 19 b) and Fig. 20 b). Note that the nonholonomic strategy does not suffer significant vibrations, while omnidirectional motion, even with small vibrations, still presents a satisfactory behavior. Table VII shows the average measured values and standard deviations (σ) for both operation modes summarizing the tests' performance.

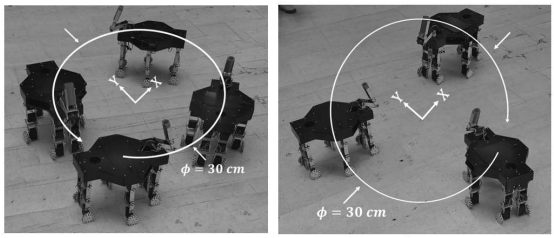

Fig. 18. Snapshot of the test for describing a circular trajectory: a) Nonholonomic motion, b) Omnidirectional motion.

TABLE VI
ANGULAR VELOCITIES FOR A CIRCULAR TRAYECTORY: NONHOLONOMIC AND OMNIDIRECTIONAL MOTIONS

Wheel	ω [rad/s] (nonholonomic)	ω [rad/s] (omnidirectional)
Left Forward Wheel (ω_1)	6.78	4.97
Left Wheel (ω_2)	2.47	-5.74
Left Backward Wheel (ω_3)	0.91	0.66
Right Forward Wheel (ω_4)	3.52	-4.97
Right Wheel (ω_5)	7.83	5.74
Right Backward Wheel (ω_6)	9.39	-0.66

TABLE VII
STATISTICAL RESULTS OF THE ROLLING IN A CURVED DISPLACEMENT TESTS.

Test mode	Max. Ψ [°]	Max. a_Z [m/s2]	Pw [W]
Nonholonomic	338.00 σ=0.097	0.20 σ=0.089	12.22 σ=0.104
Omnidirectional	324.10 σ=0.105	2.56 σ=0.099	13.43 σ=0.094

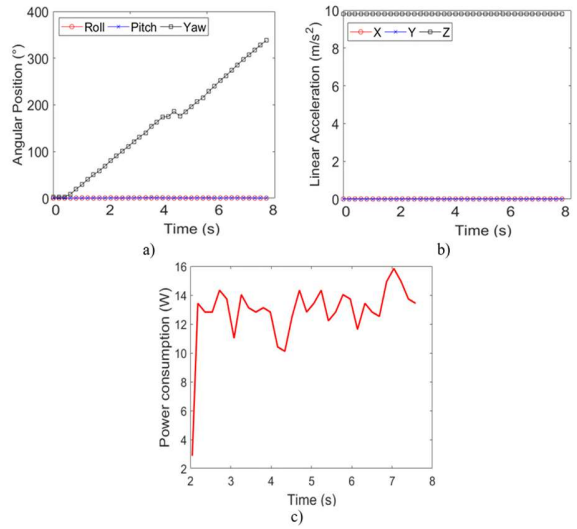

Fig. 19. Test results in a nonholonomic motion: a) Θ, Ψ, Φ ; b) a_X, a_Y, a_Z; c) power consumption.

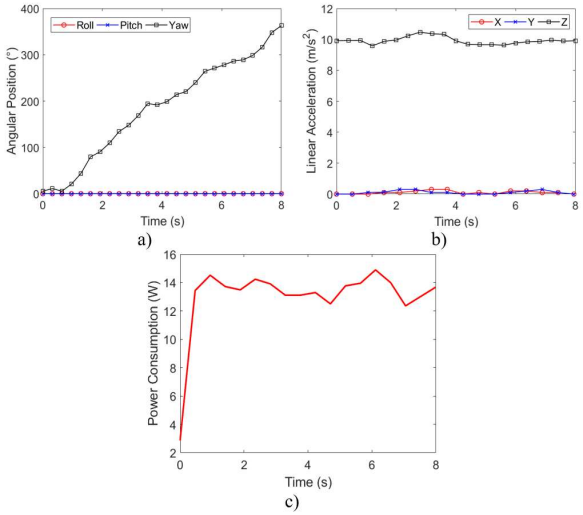

Fig. 20. Test results for omnidirectional motion: a) Θ, Ψ, Φ ; b) a_X, a_Y, a_Z; c) power consumption.

D. *Wheeled-legged Locomotion*

Wheeled-legged locomotion is implemented by considering two different situations, one where the robot is rolling, and walking to overcome small obstacles; and another one where the robot is walking and rolling.

Regarding the rolling-walking mode, the planned gait is programmed in the servo-controller of the robot. This program stores the joint angular positions of the gait, and, according to the robot velocity, determines when the robot should raise the leg to overcome the obstacle. This strategy allows to overcome obstacles of 50 mm of height and 100 mm of length. An eraser and a 3D printed cube where used as obstacles for these tests. Fig. 21 presents the sequence of the four tested

This article has been accepted for publication in a future issue of this journal, but has not been fully edited. Content may change prior to final publication. Citation information: DOI 10.1109/TMECH.2020.3027259, IEEE/ASME Transactions on Mechatronics

bio-inspired gaits. In the walking-rolling mode, the goal is to use wheels for a turn during a walk. This means that the robot can re-orientate itself by turning with the wheels during a walking mode. Fig. 22 shows a photo sequence of the test, where the robot gives two forward steps, and then turns 180° by using the wheels, and finally gives two backward steps.

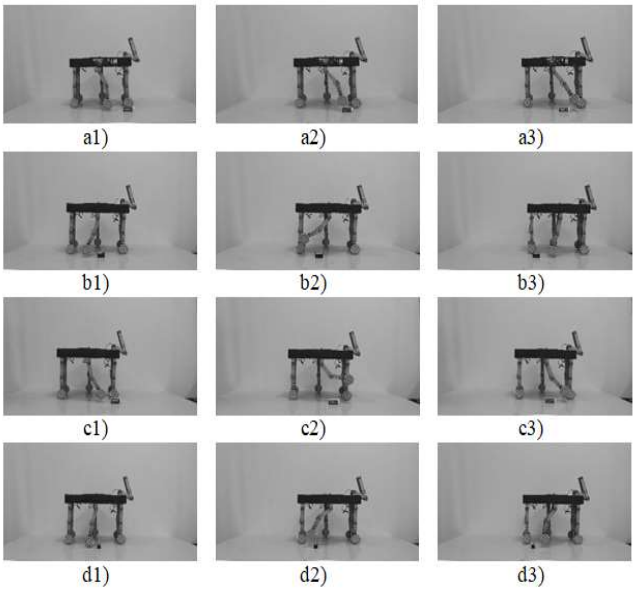

Fig. 21. Photo sequence of the tested overcoming gaits: a) human forward; b) human backward; c) bird like; d) horse like.

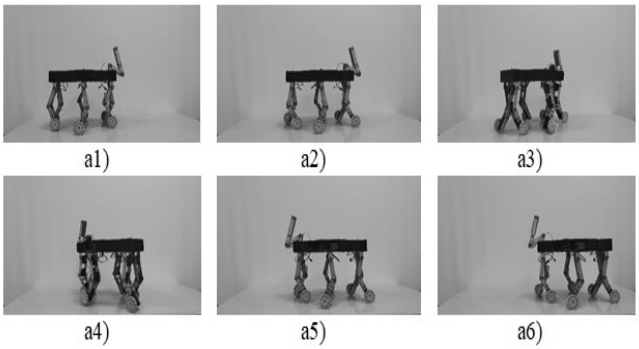

Fig. 22. Walking and turning with six wheels: a1) t = 0 s; a2) t = 4 s; a3) t = 10 s; a4) t = 12 s; a5) t = 16 s; a6) t = 20 s.

Test results of the obstacle stepping while robot is rolling are presented in Fig. 23. The final orientation error at the end of the motion is -1.8º, Fig. 23a). Linear accelerations are presented in Fig. 23b), and the power consumption is shown in Fig. 23c). One can observe that power consumption presents peaks during each step of the walking mode.

Fig. 24 presents the test results of the walking-rolling mode. One can note, in Fig. 24a), the displacement with the legs in the first eight seconds (walking); a turn of 180º with the wheels from 10 to 15 s approximately, and the last steps to reach rest configuration. One can observe vibrations appearing during the reorientation maneuver. Table VIII summarizes the statistical analysis (means values and standard deviations, σ) of these experiments. These results demonstrate the feasibility and capabilities of the hybrid wheeled-legged locomotion of Cassino Hexapod III for both displacement strategies.

TABLE VIII
STATISTICAL RESULTS OF THE WHEELED-LEGGED LOCOMOTION TESTS.

Test mode	Final angular variation in Yaw [°]	Max. linear acceleration in Z axis [m/s^2]	Average power consumption [W]
Rolling-Walking	-1.8 / σ=0.106	5.14 / σ=0.098	5.35 / σ=0.104
Walking-rolling	182.52 / σ=0.104	3.04 / σ=0.098	9.25 / σ=0.107

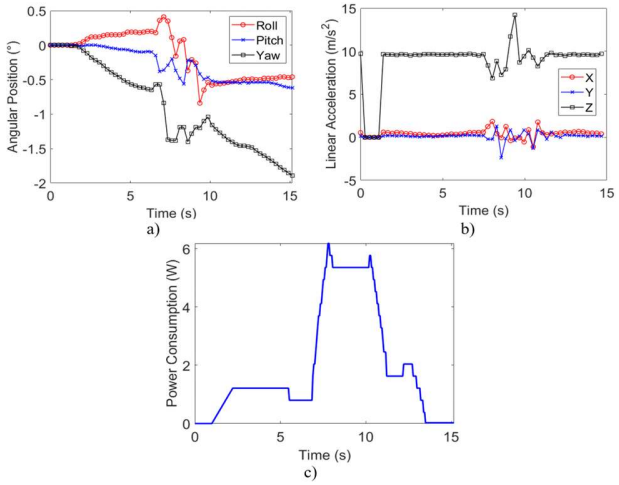

Fig. 23. Tests result for a wheeled-legged locomotion to overcome small obstacles: a) Θ, Ψ, Φ ; b) a_X, a_Y, a_Z; c) power consumption.

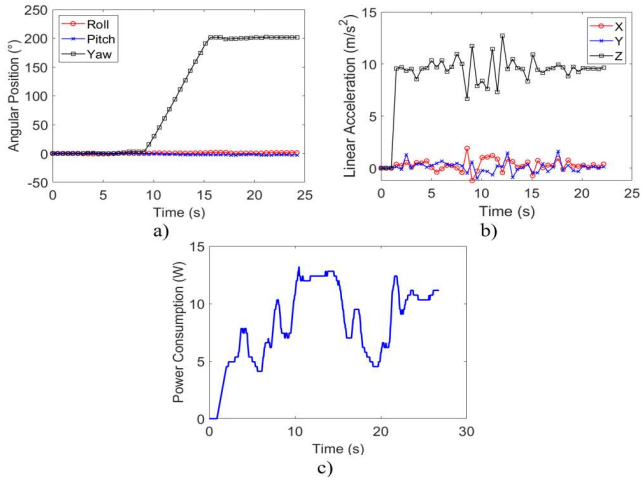

Fig. 24. Tests result for wheeled-legged locomotion to walk and turn with six wheels: a) Θ, Ψ, Φ ; b) a_X, a_Y, a_Z; c) power consumption.

VII. CONCLUSION

This paper presents a locomotion evaluation for Cassino Hexapod III, a new hybrid wheeled-legged hexapod robot that uses Mecanum-wheels. Gait planning, omnidirectional and nonholonomic rolling motions are modeled. The main contribution of this paper lies in combining such locomotion capabilities to implement various modes of operation. Each mode has been successfully tested by using wheels, legs, and legs with wheels, showing the feasibility of these locomotion strategies and the motion capabilities of the robot, in particular, for hybrid locomotion when using wheels combined with legs. This locomotion mode stands out, since it allows the robot to implement motion strategies previously not addressed in the literature. Main limitation of the current

design is given by the possibility of passive motions when negotiating inclined slopes. This aspect will be carefully addressed in future designs. There also are other strategies that need to be addressed in future works, such as rolling without stopping walking (similar to skating) and stepping over obstacles during omnidirectional movement.

ACKNOWLEDGMENT

This work was supported by the Ministry of Science and Higher Education of the Russian Federation (No. 0625-2020-0017). First author wishes to thank CONAYCT and ACRI for a grant, that supported him for a period of study at LARM.

REFERENCES

[1] R. Siegwart, I. R. Nourbakhsh, D. Scaramuzza and R. C. Arkin, Introduction to autonomous mobile robots, MIT press, 2011.
[2] M. Ceccarelli and E. F. Kececi, “Designs and Prototypes of Mobile Robots”, in Robotics Engineering Book Series, ASME PRESS, 2015.
[3] G. Carbone, and F. Gomez-Bravo (Eds.). Motion and operation planning of robotic systems: background and practical approaches (Vol. 29). Springer, 2015.
[4] B. Zhong, S. Zhang, M. Xu, Y. Zhou, T. Fang, and W. Li, "On a CPG-based hexapod robot: AmphiHex-II with variable stiffness legs." IEEE/ASME Transactions on Mechatronics, vol 23, no 2, pp. 542-551, 2018.
[5] Y. Go, X. Yin, A. Bowling, "Navigability of multi-legged robots", IEEE/ASME Trans. Mechatronics, vol. 11, no. 1, pp. 1-8, Feb. 2006.
[6] H Abdellatif, B. Heimann, "Advanced model-based control of a 6-DOF hexapod robot: A case study", IEEE/ASME Trans. Mechatronics, vol. 15, no. 2, pp. 269-279, Apr. 2010.
[7] S. Seok et al., "Design principles for energy-efficient legged locomotion and implementation on the MIT cheetah robot", IEEE/ASME Trans. Mechatronics, vol. 20, no. 3, pp. 1117-1129, Jun. 2015.
[8] G. Zhong, L. Chen, and H. Deng, "A performance oriented novel design of hexapod robots," IEEE/ASME Transactions on Mechatronics, vol 22, no 3, pp. 1435-1443, 2017.
[9] M. Hörger, N. Kottege, T. Bandyopadhyay, A. Elfes and P. Moghadam, "Real-time stabilisation for hexapod robots," in Experimental Robotics, Springer, Cham, 2016, pp. 729-744.
[10] M. Yasushi, T. Yuuya, A. Tatsuo, I. Kenji and K. Noriho, "Omni-directional Locomotion of Robots with Limb Mechanism," Journal of Robotics Society of Japan, vol. 22, no 3, pp. 329-335, 2004.
[11] E. Rohmer, G. Reina and K. Yoshida, “Dynamic Simulation-Based Action Planner for a Reconfigurable Hybrid Leg–Wheel Planetary Exploration Rover,” Advanced Robotics, vol 24, no 8-9, p 1219, 2010.
[12] F. Tedeschi and G. Carbone, "Hexapod Walking Robot Locomotion," in Motion and Operation Planning of Robotic Systems, Springer, 2015, pp. 439-468.
[13] F. Tedeschi, and G. Carbone, "Design of a novel leg-wheel hexapod walking robot," Robotics, vol 6, no 4, pp. 40-52, 2017.
[14] A. Gasparetto,P. Boscariol, A. Lanzutti and R. Vidoni, "Path Planning and Trajectory Planning Algorithms: A General Overview," in Motion and Operation Planning of Robotic Systems, Springer, 2015, pp. 3-27.
[15] Marco Ceccarelli Giuseppe Carbone, Design and Operation of Human Locomotion Systems, Elsevier Academic Press, 2019.
[16] S. M. Song and K.J. Waldron. “An analytical approach for gait study and its applications on wave gaits,” Int. J. Robot. Res., 6, 60–71, 1987.
[17] D. Belter and P. Skrzypczynski, "Integrated Motion Planning for a Hexapod Robot Walking on Rough Terrain," in Proceeding of the 18th IFAC World Congress, Milano, Italy, 2011, p. 6918-6923.
[18] K. Zimmermann, I. Zeidis and M. Abdelrahman, "Dynamics of Mechanical Systems with Mecanum Wheels," in Applied Non-Linear Dynamical Systems, Springer, Cham, 2014 pp. 271-279.
[19] P. Viboonchaicheep, A. Shimanda and Y. Kosaka, "Position rectification control for Mecanum wheeled omni-directional vehicles," in Proceedings of the 29th Annual Conference of IEEE Industrial Electronics Society, Virginia, USA, 2003, pp. 854-859.
[20] A. Gfrerrer, "Geometry and Kinematics of the Mecanum Wheel," Computer Aided Geometric Design, vol 25, no 9, pp. 784-791, 2008.
[21] F. Gomez-Bravo, M. J. Aznar-Torres and G. Carbone, "Optimal Motion for Obstacle Stepping in a Hybrid Wheeled-Legged Hexapod," in 2014 IEEE International Conference on Autonomous Robot Systems and Competitions (ICARSC), Espinho, Portugal, 2014, pp. 53-58.

Ernesto Christian Orozco-Magdaleno received his B.S. degree in Electromechanical Engineering from ITLAC (Lazaro Cardenas Institute of Technology) in 2016 and the M.S. degree on Advanced Technology from CICATA (Research Center on Applied Science and Advanced Technology), Queretaro Unit, National Polytechnic Institute, in 2018. From 2018 he is a full-time PhD student on Advanced Technology in CICATA-QRO.

Fernando Gomez-Bravo received his Licenciatura (M.S. degree) in Industrial Physic and Automatics from UNED (Madrid) 1991. In 2001 he obtained the PhD degree in Robotics and Automatics from Sevilla University. From 1991 to 2001 he was with the national railway company (RENFE). Since 2001 he is full-time professor at the Huelva University, being the responsible of the Robotic Laboratory at the Electronic Systems and Mechatronics research group. His research interests cover aspects of Robotics, Mechatronics and Motion Planning and Control. He is author or co-author of more than 80 scientific papers including journal and conference articles, book chapters and patents.

Eduardo Castillo-Castañeda received his B.S. degree with honors in Mechanical Electrical Engineering from the National Autonomous University of Mexico, in 1987. In 1988 he obtained the Diploma of Specialization at the Higher School of Electricity, in Rennes, France. He obtained his PhD degree in Automatic Control from the National Polytechnic Institute of Grenoble (France), in 1994. Currently, he is a full-time professor at CICATA (Center for Research in Applied Science and Advanced Technology), Querétaro Unit, National Polytechnic Institute, he is a member of the IPN Robotics and Mechatronics Network and of the IFToMM Technical Committee on Robotics and Mechatronics.

Giuseppe Carbone received the M.S. cum laude and PhD degree at University of Cassino (Italy) where he has been a Key Member of LARM (Laboratory of Robotics and Mechatronics) for about 20 years. Since Dec. 2018 he is Associate Professor at DIMEG, University of Calabria, Italy. His research interests cover aspects of Mechanics of Manipulation and Grasp, Mechanics of Robots, Mechanics of Machinery with more than 300 published papers. Among others, he currently serves as Chair of the IFToMM TC Robotics and Mechatronics, Member of the Board of Directors for the Society of Bionics and Biomechanics, Treasurer of the IFToMM Italy Society, Associate Editor of several International Journals.